

변형률 속도가 콘관입시험에 미치는 영향

Influence of Penetration Rate on Piezocone Penetration Test

김대규, Dae-kyu Kim

Senior Researcher, Research Center for Disaster Prevention Science and Technology, Korea University, 고려대학교 부설 방재과학기술연구센터 선임연구원

SYNOPSIS : 본 연구에서는 콘관입속도가 콘관입시험 결과에 미치는 영향을 연구하기 위하여 LSU/CALCHAS(Louisiana State University Calibration Chamber System)를 이용한 미니 Piezocone의 관입시험이 수행되었으며 그 결과를 비교 분석하였다. 10회의 미니 Piezocone 관입시험이 Ko 조건에서 수행되었으며 33% kaolin, 67% sand mixture가 시료로 사용되었고, 콘관입속도 0.3, 0.6cm/sec, U1(filter element at the cone tip), U2(filter element above the cone base), OCR=1, 10 의 조건이 다양하게 적용되었다. 시험결과 Cone Resistance, Excess Pore Water Pressure, Sleeve Friction 은 U1, U2 두 종류의 콘에 대해서 모두 관입속도가 커짐에 따라 증가하였으나 OCR의 증가에 따라서는 감소하였으며 U1의 Excess Pore Water Pressure가 U2 경우보다 크게 측정되었다.

Key Words : Penetration Rate, LSU/CALCHAS, Piezocone, Calibration Chamber

1. INTRODUCTION

The piezocone penetration test (PCPT or CPTU) is widely used for the evaluation of in-situ soil properties and site characterization. The direct data from the piezocone penetration test are cone resistance, sleeve friction, and excess pore water pressure. In addition, the change of excess pore water pressure is obtained from dissipation test that follows penetration test. Many in-situ soil properties are obtained from the data of the piezocone penetration test and the subsequent dissipation test (Tumay and Acar, 1985; Kurup, 1993; Voyiadjis, et al., 1994; Tumay, et al., 1995).

Interpretations of the data from piezocone penetration test are often complex as they are influenced by a number of variables related to the design of the cone, testing procedure, and soil characteristics (Tumay, et al., 1998; Voyiadjis, et al., 1991, 1994; Kurup, et al., 1994).

Among the many influencing factors, the rate of penetration is one of the influencing factors related to testing procedure. The standard rate of penetration test is 2cm/sec. The cone resistance tends to decrease for the penetration rate less than 2cm/sec (Acar, 1981; Campanella and Robertson, 1981). The penetration rate has also an influence on excess pore water pressure and sleeve friction (Roy, et al., 1982; Campanella and Robertson, 1981). If the mechanism of piezocone penetration needs to be theoretically analyzed, the use of viscoplasticity would be recommended since elastoplasticity alone can not account for time dependent behavior such as strain rate effect.

In this research, the influence of penetration rate on the results of piezocone penetration test, i.e., cone resistance, excess pore water pressure, and sleeve friction, has been investigated through a laboratory model test using a miniature piezocone and a well-calibrated calibration chamber.

Calibration chamber test is performed to calibrate in-situ testing devices. In a calibration chamber test, the homogeneous, reproducible, and instrumented soil specimen can be prepared with a known stress history. Therefore, various parametric studies can be performed under well-controlled boundary conditions. The facts stated above present definite advantages of the calibration chamber test in the laboratory over in-situ testing. LSU/CALCHAS (Louisiana State University Calibration Chamber System) was used in this research.

The test results, experimental equipment, and procedure are presented in the following sections.

2. Experimental Equipment and procedure

This section describes the experimental equipment and procedure of PCPT (Piezocone Penetration Test) using LSU/CALCHAS (Louisiana State University Calibration Chamber System) and the Slurry Consolidometer (Tumay and De Lima, 1992; Kurup, 1993; Kurup, et al., 1994; Voyiadjis, et al., 1993). Ten penetration tests were conducted using the miniature piezocone at the penetration rates 0.3 cm/sec and 0.6 cm/sec and for normally consolidated specimen and heavily overconsolidated (OCR=10) specimen.

The procedure of the piezocone penetration test is as the following. First, the dry soil sample is mixed with water and the soil slurry is placed in the consolidometer. After the slurry consolidation in the consolidometer, the soil specimen is moved into the calibration chamber. The piezocone penetration test is conducted after reconsolidation in the calibration chamber.

2.1 Preparation of Soil Slurry and Slurry Consolidometer

Soil slurry was prepared by mixing dry soil sample and deionized water at a water content of twice the liquid limit using a heavy duty chemical mixer (figure 1). A mixture of 33% kaolin and 67% fine sand by dry weight was used to prepare the K33 soil specimen. The grain size distributions of the kaolin, the fine sand, and the mixture are shown in figure 2.

The slurry consolidometer was designed and used to prepare large cohesive specimen by Kurup (1993) and Kurup, et al. (1994).

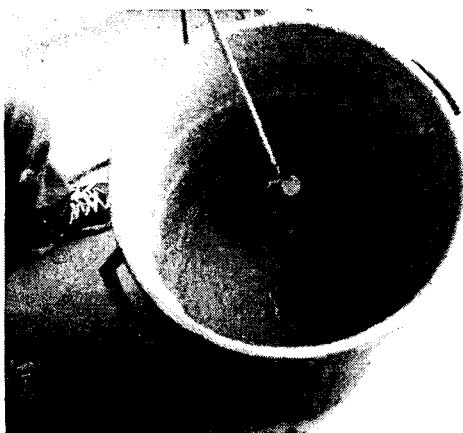


Figure 1 Soil slurry mixing

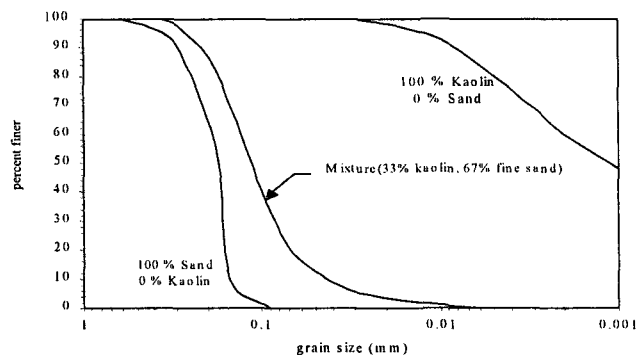


Figure 2 Grain size distribution

The slurry consolidometer is composed of two PVC tubes. Each tube is 525 mm in inside diameter, 15 mm thick, and 812 mm in height. The lower tube is split longitudinally into two halves which are held together by a metal frame to minimize disturbance of the soil specimen while transferring it into the calibration chamber (see section 2.2). Seven pore water pressure ducts, whose tips are located at various radial distances and at two different elevations, were instrumented inside the consolidometer after saturation. The ducts were saturated by flushing with deaired water and assembled with the pressure transducer in a tub of deaired water (figure 3). The tips of the ducts were immersed in deaired water and subjected to vacuum in the Nold DeAerator to ensure the saturation. They were connected to individual pressure transducers through the base plate. The tip of the duct was sealed with porous plastic filter material against the clogging of the tube.

Before pouring the soil slurry into the consolidometer, a 1.59 mm thick rubber membrane was placed inside the consolidometer to confine the specimen and the ducts were instrumented to measure the pore water pressure at appropriate heights and locations (figure 4). The soil slurry was placed very carefully inside the consolidometer, so that air bubbles might not be included in the slurry and the pore water pressure ducts instrumented inside the consolidometer are kept saturated.

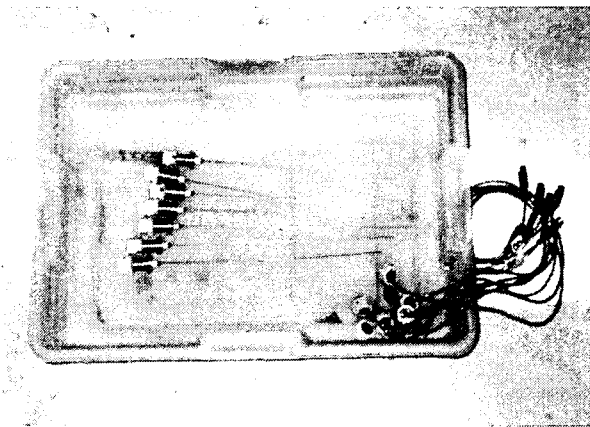


Figure 3 Pore water pressure ducts and transducers



Figure 4 Lower tube with membrane and pore water pressure ducts

2.2 Slurry Consolidation in Slurry Consolidometer

A consolidation stress of 206.85 kPa was applied to the soil slurry. This vertical stress was selected to consider the rigid boundary effect of the slurry consolidometer and to obtain an initial soil specimen of sufficient strength for self-standing. The change of pore water pressure during the consolidation in the consolidometer could be monitored from the ducts and the data acquisition system. Figure 5 shows the consolidation in the slurry consolidometer and figure 6 shows the schematic of the slurry consolidometer system. The loading system for slurry consolidation consists of a hydraulic cylinder jack powered by an air hydraulic pump and an aluminum piston plate with a steel piston rod and holes for drainage and back pressure. The load from the push jack is transferred to the soil through the piston rod and the piston plate.

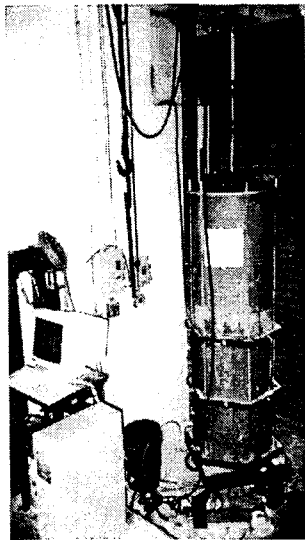


Figure 5 Consolidation in slurry consolidometer

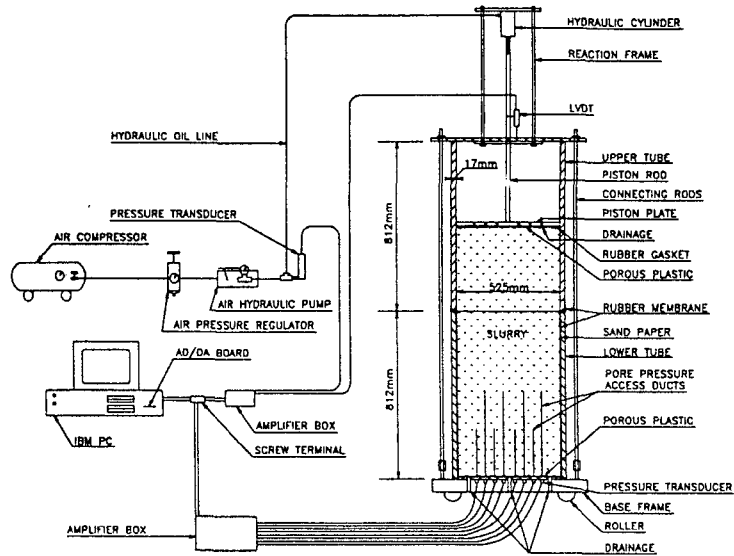


Figure 6 Schematic of slurry consolidometer system (Kurup, 1993)

2.3 Reconsolidation in Calibration Chamber

After the consolidation in the slurry consolidometer, the upper tube of the consolidometer was removed and the top surface of the specimen was trimmed at an appropriate height (figure 7). Then, the specimen was transferred into the calibration chamber using an overhead crane (figure 8). The lower tube of the slurry consolidometer was removed carefully not to disturb the specimen, and the inner shell and the outer shell of the calibration chamber were placed through the specimen. After that, the reconsolidation of the specimen was performed using LSU/CALCHAS.

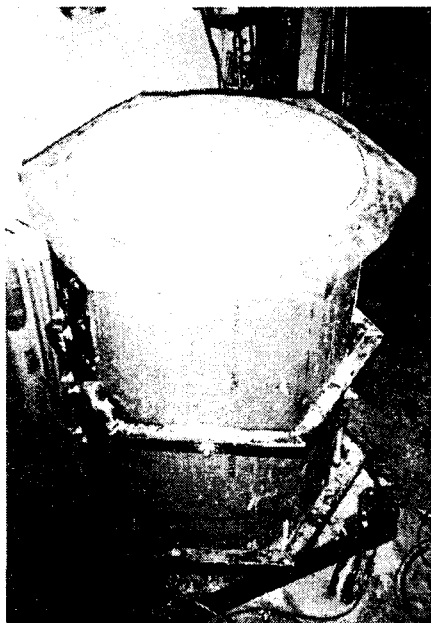


Figure 7 Specimen in consolidometer after slurry consolidation

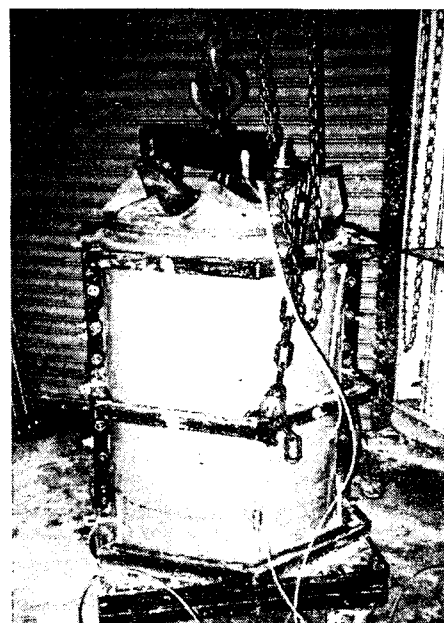


Figure 8 Transferring specimen into calibration chamber

Table 1 shows the stress conditions for reconsolidation and piezocone penetration test. Figure 9 and figure 10 show the LSU/CALCHAS.

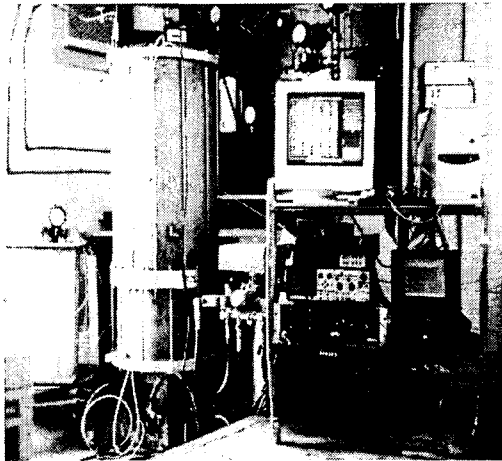


Figure 9 Reconsolidation using LSU/CALCHAS

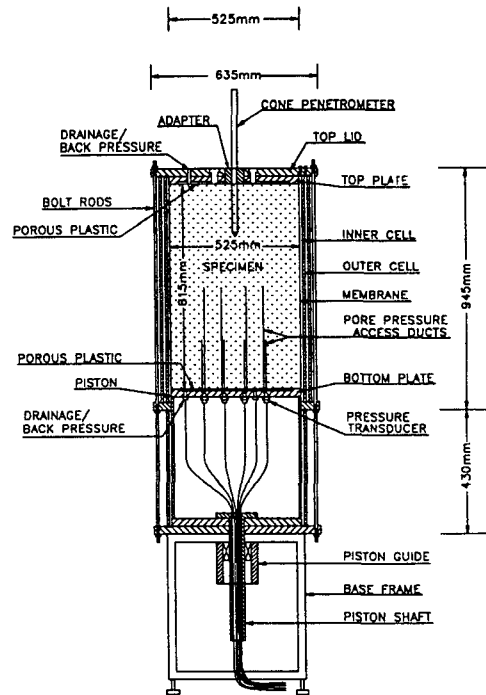


Figure 10 Schematic of flexible double wall calibration chamber (Kurup, 1993)

Table 1 Miniature piezocone penetration test program

Penetration Test no.	Filter location	sv (kPa)	sh (kPa)	Ko	OCR	Penetration Rate (cm/sec)
1	u1	262.01	110.04	0.42	1	0.3
2	u1	262.01	110.04	0.42	1	0.3
3	u2	262.01	110.04	0.42	1	0.3
4	u2	262.01	110.04	0.42	1	0.3
5	u1	262.01	110.04	0.42	1	0.6
6	u1	262.01	110.04	0.42	1	0.6
7	u2	262.01	110.04	0.42	1	0.6
8	u2	262.01	110.04	0.42	1	0.6
9	u2	26.20	41.40	1.58	10	0.6
10	u1	26.20	41.40	1.58	10	0.6

LSU/CALCHAS (Louisiana State University Calibration Chamber System) was designed by de Lima (1990), de Lima and Tumay (1991), and Tumay and de Lima (1992). It consists of a flexible

double wall chamber which makes K_0 condition possible, a piston cell, control panel, back pressure system, and data acquisition/control software. The internal diameters of the inner and outer shells of the flexible double wall chamber are 560 mm and 580 mm, respectively (figure 9 and figure 10). Deaired water was filled between the specimen and the inner shell and between the inner shell and the outer shell. The lateral stress was applied to the specimen from the double wall chamber. The double wall chamber can hold the specimen 525 mm in diameter and 815 mm high. The piston cell is also a double walled cylinder. The inner cell was kept free for instrumentation, and the outer cell between the two shells and the grooves at the bottom of the piston plate were filled with deaired water. The piston was raised to apply the vertical stress to the specimen by pressurizing the water in the piston cell. The control panel controls the vertical and lateral stresses manually or automatically. The change of pore water pressure can be monitored from the data acquisition system and the pore water pressure ducts instrumented at the beginning of the experiment. Using the equipment described above, LSU/CALCHAS can simulate various boundary conditions.

2.4 Miniature Piezocone Penetration Test

After the reconsolidation in the calibration chamber, the miniature piezocone was saturated, then penetration tests were conducted using the hydraulic and chucking system at the rates of 0.3 cm/sec and 0.6 cm/sec. Cone tip resistance, sleeve friction, pore water pressure at U1 and U2 configuration, as stated in table 1, were measured from the data acquisition system. The results of miniature piezocone penetration tests are presented in the following section.

Eight piezocone penetration tests were conducted for the normally consolidated specimen. After the penetration tests, all pressures were carefully released and the specimen was consolidated again to simulate heavily overconsolidated state ($OCR=10$). Then two additional piezocone penetration tests were conducted. Both consolidations for the normally consolidated state and for the heavily overconsolidated state were performed under K_0 condition.

The miniature piezocone penetrometer fabricated by Fugro B.V., the Netherlands, on loan to Professor Mehmet T. Tumay, was used for the tests. It has a projected cone area of 100 mm^2 , a cone apex angle of 60° , a friction sleeve area of 1526 mm^2 , and a slope sensor. The miniature piezocone penetrometer has two alternatives for the filter location. The filter can be located at the very cone tip (U1 configuration, figure 11) or at 1 mm above the base of the cone (U2 configuration, figure 12).

The filter elements of the piezocone and the transducer cavity were fully saturated (boiling and cleaning in ultra-sonic cleaner, then applying vacuum) (Juran and Tumay, 1989). The hydraulic system (for grabbing and pushing piezocone penetrometer) was mounted on the calibration chamber and the penetration and extraction of the piezocone were conducted in a single stroke of maximum 640 mm. The penetration depth was measured using the depth decoding system. All data (cone resistance, excess pore water pressure, sleeve friction, and corresponding depth) were recorded using the data acquisition system. Details regarding PCPT using LSU/CALCHAS are also described in de Lima (1990), Kurup (1993), Kim (1999), and Lim (1999)

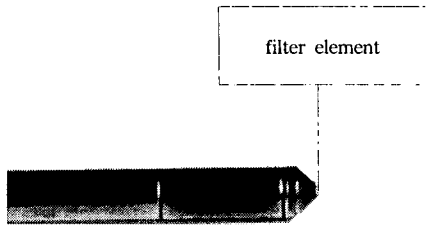


Figure 11 U1 configuration

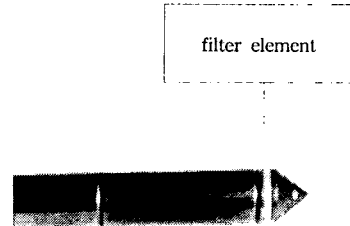


Figure 12 U2 configuration

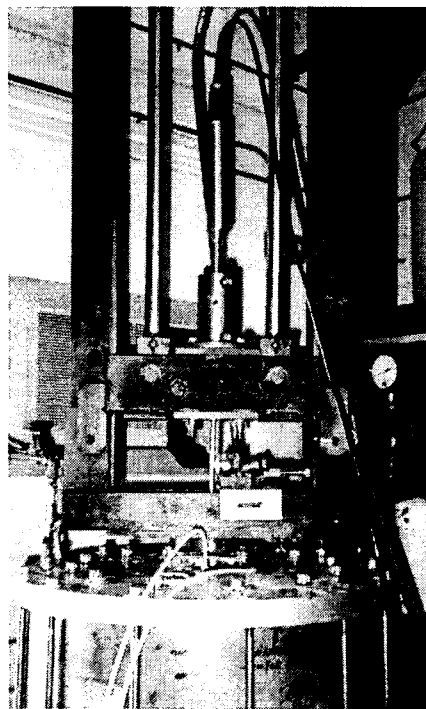


Figure 13 Piezocone penetration test

3. Test Result

In this section, the results of the penetration tests (cone resistance, excess pore water pressure, sleeve friction) are presented. As shown in the miniature piezocone penetration test program (table 1), the penetration test no.2, no.4, no.6, and no.8 are the replications of the penetration test no.1, no.3, no.5, and no.7, respectively. The replications have been conducted to confirm the reliability of the test results. The maximum difference between the results of the tests and the results of the replications were less than 9 %, so only the averages are presented. The averages of penetration test no.1 and no.2 are expressed as 0.3 cm/sec (U1, NC), which means the penetration test conducted using U1 configuration piezocone and normally consolidated sample at the penetration rate

of 0.3 cm/sec. Similarly, the averages of the penetration test no.3 and no.4, no.5 and no.6, and no.7 and no.8 are expressed as 0.3 cm/sec (U2, NC), 0.6 cm/sec (U1, NC), and 0.6 cm/sec (U2, NC), respectively. The 0.6 cm/sec (U2, OCR=10) indicates the penetration test no.9. The 0.6 cm/sec (U1, OCR=10) means the test no.10. The U1 configuration is the piezocone with the filter element located at the cone tip and the U2 configuration has the filter element 1mm above the cone base as described in section 2.4. Test no.9 and test no.10 have been conducted at the same location. Test no.9 (0.6 cm/sec, U2, OCR=10) has been conducted to the penetration depth of 220 mm. After the dissipation test of test no.9, the penetration test of test no.10 (0.6 cm/sec, U1, OCR=10) was performed from 0 mm depth to 580 mm depth at the same location. So, the profile from 0 mm to 220 mm of test no.10 (dotted line portion of 0.6 cm/sec, U1, OCR=10 in figure 14, figure 15, and figure 16) has no practical relevance and the profile below the depth of 220 mm (real line portion of 0.6 cm/sec, U1, OCR=10 in figure 14, figure 15, and figure 16) was used.

3.1 Cone Resistance

The cone resistance was expressed as the corrected cone resistance, q_T , and back pressure, u_0 . The corrected cone resistance was obtained from the measured cone resistance and the pore water pressure measured behind the cone tip (Tumay and Acar, 1985; Kurup, 1993). The area ratio of the miniature piezocone used in this research was 0.62. Figure 14 shows the cone resistance profiles from the piezocone penetration tests.

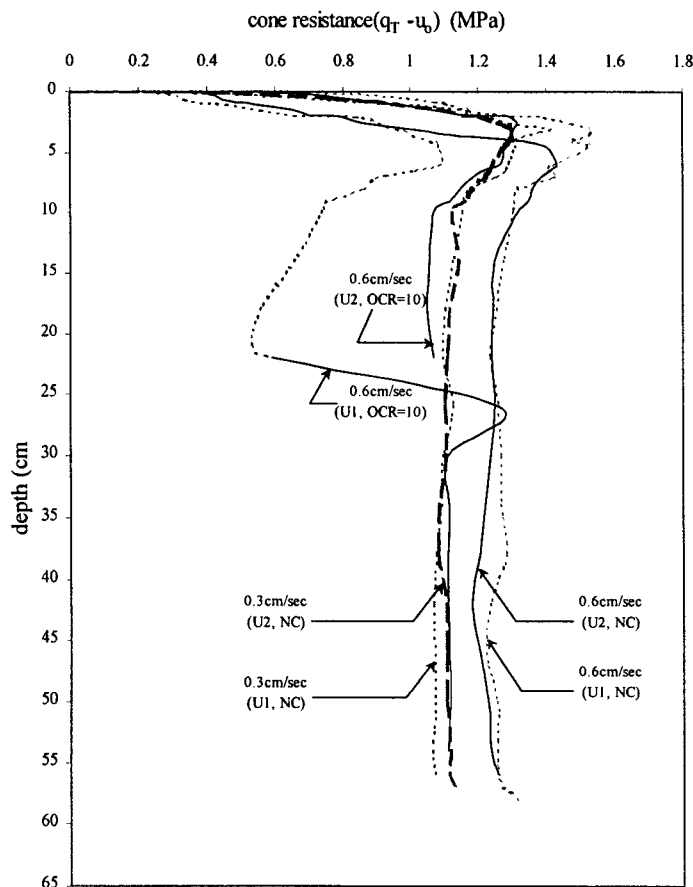


Figure 14 Cone resistance profiles

As shown in figure 14, the steady values of cone resistances for 0.6 cm/sec (U1, NC) and 0.6 cm/sec (U2, NC) were almost same (1.23 MPa), and the corresponding penetration depths were also almost same (140 mm). The steady values of cone resistance both for 0.3 cm/sec (U1, NC) and for 0.3 cm/sec (U2, NC) were 1.12 MPa, and the corresponding depths were 105 mm. Accordingly, it can be said that the steady value of cone resistance and the corresponding depth are equal regardless of the location of filter element, i.e., U1 or U2 configuration. The steady values of cone resistances for 0.6 cm/sec (U1, OCR=10) and 0.6 cm/sec (U2, OCR=10) were 1.11 MPa and 1.04 MPa, respectively.

By comparing the steady values of 0.3 cm/sec (U1 and U2, NC) with those of 0.6 (U1 and U1, NC), the penetration rate effects on cone resistance can be shown. The penetration tests were conducted under the same stress conditions, and only the penetration rates were different. It has been found that the cone resistances at higher penetration rate were larger than those at lower rate. In this research, more specifically, the steady value of cone resistance at 0.3 cm/sec increased by 10 % with 100 % increase in penetration rate both for U1 and U2 configurations.

When the confining stresses decreased, keeping the other conditions unchanged, namely, comparing the cone resistances of 0.6 cm/sec (U1 and U2, NC) with those of 0.6 cm/sec (U1 and U2, OCR=10), the steady value of cone resistance decreased to 13% with the increase of OCR from 1 to 10.

3.2 Excess Pore Water Pressure

Figure 15 shows the excess pore water pressure profiles of the piezocone penetration tests. As shown in figure 15, the steady values of excess pore water pressures for 0.6 cm/sec (U1, NC), 0.6 cm/sec (U2, NC), 0.3 cm/sec (U1, NC), 0.3 cm/sec (U2, NC), 0.6 cm/sec (U1, OCR=10), and 0.6 cm/sec (U2, OCR=10) were 0.086 MPa, 0.081 MPa, 0.067 MPa, 0.064 MPa, 0.063 MPa, and 0.053 MPa, respectively.

In all cases tested under the same stress condition (NC or OCR=10) and at the same penetration rate (0.3 cm/sec or 0.6 cm/sec), it was clearly observed that the excess pore water pressures measured at the cone tip (U1 configuration) were greater than those measured above the cone base (U2 configuration) unlike in the cone resistance profiles. This can be explained by that the soil below the cone tip is subjected to predominantly normal stress, on the other hand, the soil above the cone base mainly experiences shear stress, so even negative excess pore water pressures are often recorded just above the cone base for stiff overconsolidated clays (Tumay, et al., 1982; Kurup, 1993; Kurup, et al., 1994).

The differences between the excess pore water pressures of U1 configurations and those of U2 configuration for 0.3 cm/sec (NC), 0.6 cm/sec (NC), and 0.6 cm/sec (OCR=10) were 4.5 %, 5.8 %, and 15.9 %, respectively. So, it can be said that the difference of the excess pore water pressures between U1 and U2 configurations increases with the increase of penetration rate and it also increases with the increase of OCR.

By comparing the excess pore water pressures for 0.3 cm/sec (U1 or U2, NC) with those for 0.6 cm/sec (U1 or U2, NC), the penetration rate effects on excess pore water pressure can be found. With respect to U1 configuration, 22 % increase of excess pore water pressure has been found with the increase of penetration rate from 0.3 cm/sec to 0.6 cm/sec. With respect to U2 configuration, 21 % increase of excess pore water pressure has been found with the increase of penetration rate from 0.3 cm/sec to 0.6 cm/sec. This means that excess pore water pressures measured both at the cone

tip and above the cone base increase with the increase of penetration rate at a very similar rate.

The effects of OCR on excess pore water pressure can be shown by comparing the results of 0.6 cm/sec (U1 and U2, NC) with those of 0.6 cm/sec (U1 and U2, OCR=10). The 27 % and 33 % decreases of excess pore water pressures have been found with the increase of OCR from 1 to 10 for U1 and U2 configurations, respectively, which means the decrease of excess pore water pressure in U2 configuration is greater than that in U1 configuration with the increase of OCR.

3.3 Sleeve Friction

Figure 16 shows the sleeve friction profiles obtained from the penetration tests.

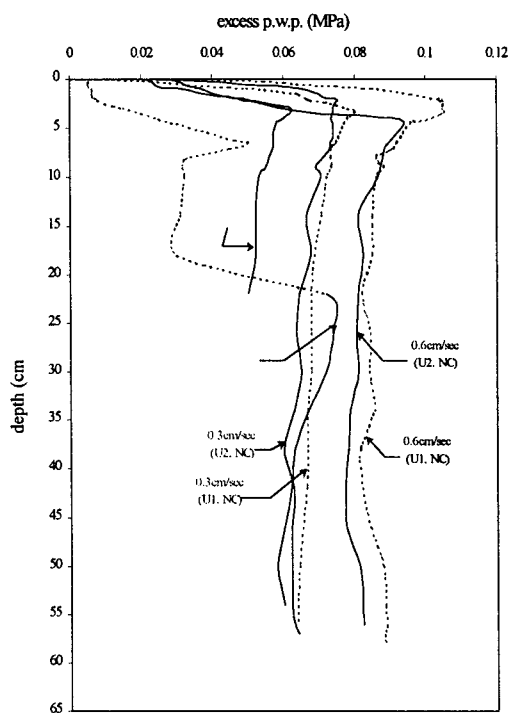


Figure 15 Excess pore water pressure profiles

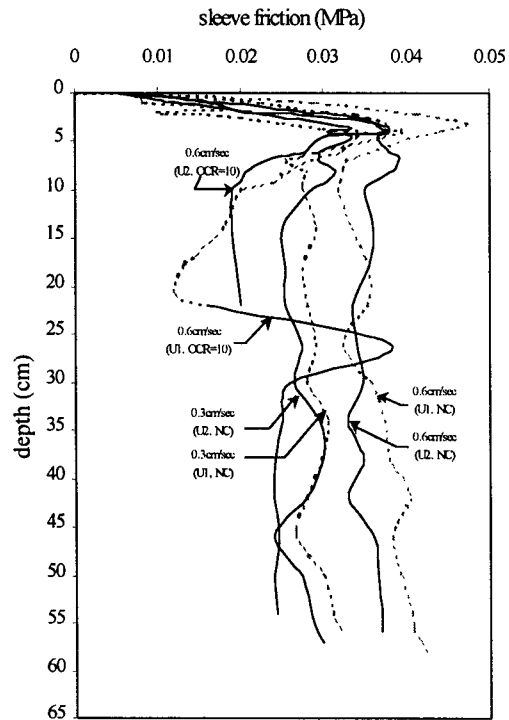


Figure 16 Sleeve friction profiles

The sleeve friction was not stable as cone resistance and pore water pressure, but the effects of penetration rate and OCR on sleeve friction were clearly shown in figure 16.

The steady values for 0.3 cm/sec (U1, NC), 0.3 cm/sec (U2, NC), 0.6 cm/sec (U1, NC), 0.6 cm/sec (U2, NC), 0.6 cm/sec (U1, OCR=10), and 0.6 cm/sec (U2, OCR=10) could be estimated to be 0.028 MPa, 0.027 MPa, 0.034 MPa, 0.034 MPa, 0.024 MPa, and 0.020 MPa, respectively.

For all cases, the steady values of U1 configurations were quite close to those of U2 configurations except for 0.6 cm/sec (OCR=10).

The steady values of sleeve frictions increased to 18 % and 21 % for U1 and U2 configurations, respectively, with the increase of the penetration rate from 0.3 cm/sec to 0.6 cm/sec. The steady values of 0.6 cm/sec (NC) decreased to 29 % and 41% for U1 and U2 configurations, respectively, with the increase of OCR from 1 to 10.

From the facts stated above, it can be said that the sleeve friction increases with the increase of penetration rate, but decreases with the increase of OCR, like cone resistance and excess pore water pressure.

4. Conclusions

In this research, the influence of penetration rate, OCR, and filter element on cone resistance, excess pore water pressure, and sleeve friction of piezocone penetration test results were investigated through ten miniature piezocone penetration tests conducted using LSU/CALCHAS and under K_0 condition. From the test results, the following conclusions can be made.

- 1 The corrected cone resistance, q_T , at the steady state and the required depth were not influenced by the location of the filter element.
- 2 The cone resistance increased with the increase in penetration rate, but decreased with the increase of OCR.
- 3 The excess pore water pressures measured at the cone tip (U1 configuration) was greater than that measured above the cone base (U2 configuration), unlike the cone resistance.
- 4 The difference of the excess pore water pressures between U1 and U2 configurations increased with the increase of penetration rate and with the increase of OCR.
- 5 The excess pore water pressures measured both at the cone tip and above the cone base increased with the increase of penetration rate at a very similar rate.
- 6 The decrease of excess pore water pressure for U1 configuration was greater than that for U2 configuration with the increase of OCR.
- 7 The measured sleeve friction was not as stable as cone resistance and excess pore water pressure.
- 8 The sleeve friction increased with the increase of penetration rate, but decreased with the increase of OCR, as did cone resistance and excess pore water pressure.
- 9 More piezocone penetration tests need to be conducted at various penetration rates other than 0.3 cm/sec and 0.6 cm/sec, and for various OCR values and soil compositions.

5. REFERENCES

- 1 Campanella, R. G. and Robertson, P. K., 1981, "Applied Cone Research," in Cone Penetration Testing and Experience, Ed. R.M. Norris and R. D. Holtz, ASCE, New York, NY, pp. 343-362
- 2 de Lima, D. C., 1990, "Development, Fabrication and Verification of the LSU In-Situ Testing Calibration Chamber," Ph.D. Dissertation, Louisiana State University, Baton Rouge, LA, 340 pp.
- 3 Juran, I. and Tumay, M.T., 1989, "Soil Stratification using the Dual Pore-Pressure Piezocone Test", Transportation Research Record, No. 1235, pp.68-78
- 4 Kim, Daekyu, 1999, "Numerical Simulation and Experimental Verification of Cone Penetration Rate and Anisotropy in Cohesive Soils", Ph.D. Dissertation, Dept. of Civil and Environmental Engineering, Louisiana State University, Baton Rouge, LA.
- 5 Kurup, P. U., 1993, "Calibration Chamber Studies of Miniature Piezocone Penetration Tests in Cohesive Soil Specimens," Ph. D. Dissertation, Department of Civil and Environmental Engineering, LSU
- 6 Kurup, P. U., Voyiadjis, G. Z., and Tumay, M. T., 1994a, "Calibration Chamber Studies of Piezocone Test in Cohesive Soils," ASCE, Journal of Geotechnical Engineering, Vol. 120, No. 1, pp. 81-107
- 7 Lim, Beyeongseock, 1999, "Determination of Consolidation Characteristics in Fine Grained Soils Evaluated by Piezocone Tests," Ph.D. Dissertation, Department of Civil and Environmental

Engineering, LSU.

- 8 Roy, M., Tremblay, M., Tavenals, F., and La Rochelle, P., 1982, "Development of Pore Pressures in Quasi-Static Penetration Tests in Sensitive Clay," *Canadian Geotechnical Journal*, Vol. 19, pp. 124-138
- 9 Tumay, M. T. and Acar, Y. B., 1985, "Piezocone Penetration Testing in Soft Cohesive Soils," ASTM, STP 883, R. C. Chaney and K. R. Demars, Eds, pp. 72-82
- 10 Tumay, M. T., Acar, Y., Deseze, E. and Yilmaz, R., 1982, "Soil Exploration in Soft Clays with the Quasi-Static Electric Cone Penetrometer," *Proceedings of the Second European Symposium on Penetration Testing*, Amsterdam, pp. 915-921
- 11 Tumay, M. T. and de Lima, D. C., 1992, "Calibration and Implementation of Miniature Electric Cone Penetrometer and Development, Fabrication and Verification of the LSU in situ Testing Calibration Chamber (LSU/CALCHAS)," Department of Civil Engineering, LSU, Report No. GE-92/08
- 12 Tumay, M. T., Kurup, P. U., and Boggess, R. L., 1998, "A Continuous Intrusion of Electronic Miniature Cone Penetration Test System for Site Characterization," *Proceedings of 1st international conference on site characterization -ISC'98*, Atlanta, pp. 1183-1188
- 13 Tumay, M. T., Kurup, P. U., and Voyiadjis, G. Z., 1995, "Profiling OCR and K_o from Piezocone Penetration Tests," *International Symposium on Cone Penetration Testing*, Sweden, pp. 337-342.
- 14 Voyiadjis, G. Z., Kurup, P. U., and Tumay, M. T., 1993, "Preparation of Large-Size Cohesive Specimens for Calibration Chamber Testing," *Geotechnical Testing Journal*, GTJODJ, Vol. 16, No. 3, pp. 339-349
- 15 Voyiadjis, G. Z., Kurup, P. U., and Tumay, M. T., 1994, "Determination of Soil Properties from Laboratory Piezocone Penetration Tests," XIII ICSMFE, India, pp. 303-308
- 16 Voyiadjis, G. Z., Tumay, M. T., and Kurup, P. U., 1991, "Miniature Piezocone Penetration Tests on Soft Soils in a Calibration Chamber System," *Proceedings, ISOCCT 1*, in *Calibration Chamber Testing*, Ed. A. B. Huang, Elsevier Publishers, New York